

Thermodynamics and dynamics of the two-scale spherically symmetric Jagla ramp model of anomalous liquids

Limei Xu,¹ Sergey V. Buldyrev,^{2,1} C. Austen Angell,³ and H. Eugene Stanley¹

¹*Center for Polymer Studies and Department of Physics, Boston University, Boston, Massachusetts, 02215 USA*

²*Department of Physics, Yeshiva University, 500 West 185th Street, New York, NY 10033 USA*

³*Department of Chemistry, Arizona State University, Tempe, Arizona 85287 USA*

(Received 2 May 2006; published 11 September 2006)

Using molecular dynamics simulations, we study the Jagla model of a liquid which consists of particles interacting via a spherically symmetric two-scale potential with both repulsive and attractive ramps. This potential displays anomalies similar to those found in liquid water, namely expansion upon cooling and an increase of diffusivity upon compression, as well as a liquid-liquid (LL) phase transition in the region of the phase diagram accessible to simulations. The LL coexistence line, unlike in tetrahedrally coordinated liquids, has a positive slope, because of the Clapeyron relation, corresponding to the fact that the high density phase (HDL) is more ordered than low density phase (LDL). When we cool the system at constant pressure above the critical pressure, the thermodynamic properties rapidly change from those of LDL-like to those of HDL-like upon crossing the Widom line. The temperature dependence of the diffusivity also changes rapidly in the vicinity of the Widom line, namely the slope of the Arrhenius plot sharply increases upon entering the HDL domain. The properties of the glass transition are different in the two phases, suggesting that the less ordered phase is fragile, while the more ordered phase is strong, which is consistent with the behavior of tetrahedrally coordinated liquids such as water silica, silicon, and BeF₂.

DOI: [10.1103/PhysRevE.74.031108](https://doi.org/10.1103/PhysRevE.74.031108)

PACS number(s): 05.40.-a

I. INTRODUCTION

An open question of general interest concerning liquid water is the relation between a liquid-liquid (LL) phase transition and the dynamic properties [1–9]. The LL phase transition may have a strong effect on the dynamic properties of supercooled water, including the glass transition [10,11]. In deeply supercooled states, some glass-formers show “strong” behavior with a well-defined activation energy, while other glass-formers display “fragile” behavior [12]. Water appears to show a crossover between fragile behavior at high T to strong behavior at low T [13–17]. The recent study on the Stillinger-Weber model of silicon [18], which confirms the LL phase transition, suggests that the less ordered high-density liquid (HDL) is fragile, while the more ordered low-density liquid (LDL) is strong. These authors observed a power-law singularity of the diffusivity in the less ordered HDL phase as it approaches the spinodal of the LL transition at constant pressure. Recently the fragility transition in nanoconfined water was studied in neutron scattering experiments pioneered by the Chen group at Massachusetts Institute of Technology (MIT) [3,4], who found that water appears to show a crossover between non-Arrhenius (“fragile”) behavior at high T to Arrhenius (“strong”) behavior at low T [3,4,13,14]. Their findings were confirmed using nuclear magnetic resonance (NMR) by Mallamace *et al.* [6]. This dynamic crossover has been interpreted [5] in terms of crossing the Widom line, which is the locus of maximum correlation length in the one-phase region. Crossing the Widom line has also been related to a breakdown of the Stokes-Einstein relation [19] and a change in the hydrogen bond network [20]. This interpretation has also been offered [9] as an explanation for the observed dynamic crossover in hydrated protein [7] and DNA [8].

A set of realistic water models—ST2, TIP5P, TIP4P, TIP3P, and SPC/E—with progressively decreasing tetrahedrality which bracket the behavior of real water have been studied to explore the generic mechanisms of LL phase transition and anomalies associated with it [1,2,5,21–28]. Studies [29–35] show that tetrahedrality is not a necessary condition for anomalous behavior and several spherically symmetric potentials are indeed able to generate density and/or diffusion anomalies.

Following the pioneering work of Stell and Hemmer [36], spherically symmetric potentials with two different length scales has been widely used to model systems with LL phase transitions [5,31–33,37,38]. A simple model [Fig. 1], based on spherically symmetric soft-core potentials with both attractive and repulsive parts, was introduced by Jagla [32], who showed that it has both waterlike anomalies and a LL phase transition. Using extensive molecular dynamics (MD) simulations, we study the static and dynamics properties of this model. We find that besides the waterlike behavior found by Jagla, the simple Jagla ramp potential also exhibits a diffusivity anomaly as well as structural anomaly [39]. We further explore the dynamic behavior along different constant pressure paths in HDL (more ordered) and LDL (less ordered) phase. We observe a non-Arrhenius behavior in the LDL and Arrhenius behavior in the HDL phase, as well as a dynamic crossover which occurs above the LL critical point as the system is cooled down along constant pressure paths. This dynamic crossover has been interpreted in terms of crossing the Widom line [5], the locus of maximum correlation length in the one phase region along the extension of the liquid-liquid coexistence line. The behavior of thermodynamic response functions (constant pressure specific heat C_p and constant temperature compressibility K_T) and the structural order parameters, Q_6 (orientational)

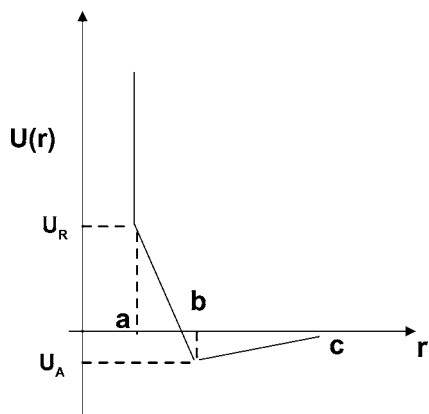


FIG. 1. (a) The spherically symmetric “two-scale” Jagla ramp potential with attractive and repulsive ramps. Here $U_R=3.5U_0$, $U_A=-U_0$, and the two length scales are a , the hard core diameter, and $b=1.72a$, the soft core diameter, while $c=3a$ is the long distance cutoff.

and t (translational), supports a relation between the dynamic crossover and the LL phase transition.

The outline of the paper is as follows. In Sec. II, we describe the spherically symmetric Jagla ramp potential. In Sec. III, we describe the method of the MD simulation. In Sec. IV, we define the quantities which we study. In Sec. V,

we investigate the static properties of the model, while Sec. VI contains the simulation results of the dynamic properties. Section VII compares the properties of Jagla model with water and another tetrahedral liquid, BeF₂.

II. SPHERICALLY SYMMETRIC TWO-SCALE JAGLA RAMP POTENTIAL

Here, we study the linear ramp potential but with both attractive and repulsive parts [32]. The potential is defined

$$U(r) = \begin{cases} \infty & r < a, \\ U_A + (U_A - U_R)(r - b)/(b - a) & a < r < b, \\ U_A(c - r)/(c - b) & b < r < c, \\ 0 & r > c, \end{cases} \quad (1)$$

where $U_R=3.5U_0$ is the repulsive energy, $U_A=-U_0$ is the attractive part, a is the hardcore diameter, $b=1.72a$ is the well minimum, and $c=3a$ is the cutoff at large distance [Fig. 1].

III. METHODS

We apply the discrete MD method [33,35], approximating the continuous potential Eq. (1) by step functions,

$$U_n(r) = \begin{cases} \infty & r < a, \\ U_R - (k - 1)\Delta U_1 & a + (k - 1)\Delta r < r < a + k\Delta r, 1 \leq k \leq n_1, \\ U_A & b < r < b', \\ U_A + k\Delta U_2 & b' + (k - 1)\Delta r' < r < b' + k\Delta r', 1 \leq k \leq n_2, \\ 0 & r > c', \end{cases} \quad (2)$$

where $\Delta r \equiv 0.02a$, $\Delta r' \equiv 0.16a$, $b' = b + 1/2\Delta r'$, $c' = c - 1/2\Delta r'$, $\Delta U_1 = (U_R - U_0)/n_1$ with $n_1 = 36$, and $\Delta U_2 = U_0/n_2$ with $n_2 = 8$.

The standard discrete MD algorithm has been implemented for particles interacting with step potentials [35,37,40–43]. We use a as the unit of length, particle mass m as the unit of mass, and U_0 as the unit of energy. The simulation time is therefore measured in units of $a\sqrt{m/U_0}$, temperature in units of U_0/k_B , pressure in units of U_0/a^3 , and density $\rho \equiv N/L^3$ in unit of a^{-3} , here L is the size of the system and $N=1728$ is the number of particles.

We implement constant volume simulations (NVT ensemble) and constant pressure simulations (NPT ensemble) in our study [23,41]. A modified Berendsen method [44] is applied to rescale the velocities of all particles for the NVT ensemble [23,41], so that the average kinetic energy per particle approaches the desired value $3KT_0/2$ where T_0 is the temperature of the thermostat according to equation

$$T' = \bar{T}(1 - \kappa_T \Delta t) + T_0 \kappa_T \Delta t, \quad (3)$$

where $\kappa_T=0.01$ is a heat exchange coefficient, Δt is the time interval during which N collisions happens, T' is the new temperature, and \bar{T} is the average temperature during the time interval Δt . For the NPT ensemble, the Berendsen algorithm rescales the coordinates \vec{r}_j and box vectors \vec{L} after each $\Delta\tau_p$ time unit:

$$\begin{aligned} \vec{r}'_j &= \vec{r}_j + \vec{r}_j \kappa_p (\bar{P} - P_0), \\ \vec{L} &= \vec{L} + \vec{L} \kappa_p (\bar{P} - P_0), \end{aligned} \quad (4)$$

where P_0 is the desired pressure, \bar{P} is the average pressure during time interval $\Delta\tau_p=10\Delta t$, $\kappa_p=1$ is the rescaling coefficient.

IV. THE FOUR QUANTITIES STUDIED

(a) The diffusion coefficient is defined as follows:

$$D \equiv \lim_{t \rightarrow \infty} \frac{\langle [\vec{r}_j(t') + t] - \vec{r}_j(t') \rangle_{t'}}{6t}, \quad (5)$$

where $\vec{r}_j(t)$ is the coordinates of particle j at time t , and $\langle \dots \rangle_{t'}$ denotes an average over all particles and over all t' .

(b) The static structure factor for wave vector \vec{q} is $S(\vec{q}) = F(\vec{q}, t=0)$, where $F(\vec{q}, t)$ is the intermediate scattering function defined as follows:

$$F(\vec{q}, t) \equiv \langle \rho(\vec{q}, t) \rho(-\vec{q}, 0) \rangle, \quad (6)$$

where $\rho(\vec{q}, t)$ is the Fourier transform of the density

$$\rho(\vec{q}, t) \equiv \sum_{j=1}^N \exp[-i\vec{q} \cdot \vec{r}_j(t)]. \quad (7)$$

(c) The translational order parameter [39,45] is defined as follows:

$$t \equiv \int_0^{r_c} |g(r) - 1| dr, \quad (8)$$

where r is the radial distance, $g(r)$ is the pair correlation function, and $r_c = L/2$ is the cutoff distance. A change in the translational order parameter indicates a change in the structure of the system. For uncorrelated systems, the interaction in the system is short ranged with $g(r) = 1$, leading to $t = 0$; for long-range correlated systems, the modulations in $g(r)$ persist over large distances, causing t to grow.

(d) The orientational order parameter Q characterizing the average local order of the i th particle [45] is defined

$$Q_{\ell,i} \equiv \left[\frac{4\pi}{2\ell+1} \sum_{m=-\ell}^{m=\ell} |\bar{Y}_{\ell,m}|^2 \right]^{1/2}, \quad (9)$$

where $\bar{Y}_{\ell,m}(\theta, \phi)$ denotes the average of the spherical harmonic function, $Y_{\ell,m}(\theta, \phi)$ with angles θ and ϕ , over the 12 bonds associated with particle i . The orientational order parameter for the entire system is calculated as follows:

$$Q_\ell = \langle Q_{\ell,i} \rangle, \quad (10)$$

where $\langle \dots \rangle$ denotes the average over all particles in the system. In general, for $\ell = 6$, the value of Q_6 increases as the local order of a system increases, e.g., $Q_6 = 0.574$ for the fcc lattice and $Q_6 = 0.289$ for uncorrelated systems.

V. SIMULATION RESULTS: STATICS

A. Equation of state

The equation of state of the Jagla ramp model [Fig. 2] is obtained using two steps: (i) constant volume simulation with slowly cooling rate $\kappa_T = 10^{-5}$, which allows us to obtain the equation of an isochore in a single run; (ii) constant temperature (NVT -ensemble) simulation of individual state points of a particular interest with heat exchange rate $\kappa_T = 0.01$. The spinodals are defined by the crossing of isochores $P(T, \rho)$ and $P(T, \rho + \Delta\rho)$, where

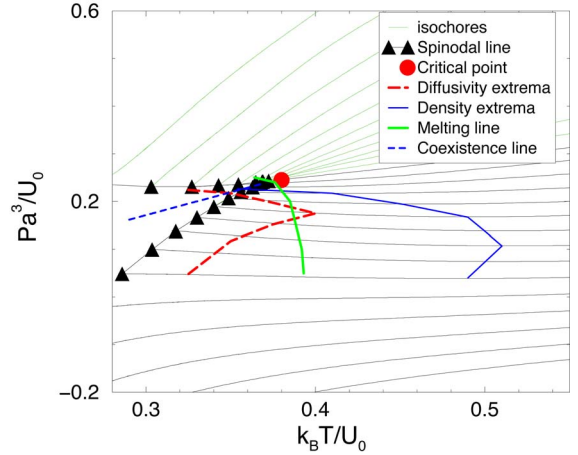


FIG. 2. (Color online) The equation of state $P(T, \rho_0)$ of the two-scale Jagla ramp potential for 26 values of density $\rho_0 \equiv Na^3/L^3$, where $L/a = 15.0, 15.2, 15.4, \dots, 20.0$ are the cell edges and $N = 1728$ is the number of particles. The LL critical point is located at $T_c = 0.375$, $P_c = 0.243$, and $\rho_c = 0.37$, above the equilibrium melting line. The gas-liquid critical point, not shown, is located at much higher temperature $T_{gl} = 1.446$ ($P_{gl} = 0.0417$ and $\rho_{gl} = 0.102$). The temperature of maximum density line is drawn by connecting all the points with $(\partial\rho/\partial T)_P = 0$, which bounds the region of the diffusivity anomaly.

$$\left(\frac{\partial P}{\partial \rho} \right)_T = 0. \quad (11)$$

To investigate the existence of the spinodals, we implement another approach, constant pressure simulation (NPT ensemble). We study the hysteresis of volume [Fig. 3(a)] and enthalpy [Fig. 3(b)] upon compression and decompression along constant temperature $T = 0.34$, and the hysteresis of volume [Fig. 3(c), 3(e), and 3(g),] and enthalpy [Fig. 3(d), 3(f), and 3(h),] upon heating and cooling along constant pressure. The volume per particle and enthalpy per particle change sharply as the system crosses the spinodal lines. There is no such sharp change in volume per particle and enthalpy per particle as we cool the system along constant pressure $P \leq 0.23$ [Fig. 3(c)] since the LDL spinodal line lies above $P = 0.23$, and thus the system remains in the LDL phase. The LL critical point, with $T_c = 0.375$, $P_c = 0.243$, and $\rho_c = 0.37$, is located at the maximal temperature on the spinodals. The coexistence line, obtained by the Maxwell rule by integrating the isotherms, has a positive slope of $0.96 \pm 0.02 k_B a^{-3}$.

According to the Clapeyron equation

$$\frac{dP}{dT} = \frac{\Delta S}{\Delta V}, \quad (12)$$

the entropy in the HDL phase is lower than the entropy in the LDL phase. Hence, the HDL phase is more ordered than the LDL phase, which is the opposite of the LL transition found in simulations for water [2] and silicon [16].

We also study the spontaneous liquid-liquid phase transition using NPT ensemble [Fig. 4]. Simulations of the isobaric heating of the HDL liquid below the critical point show

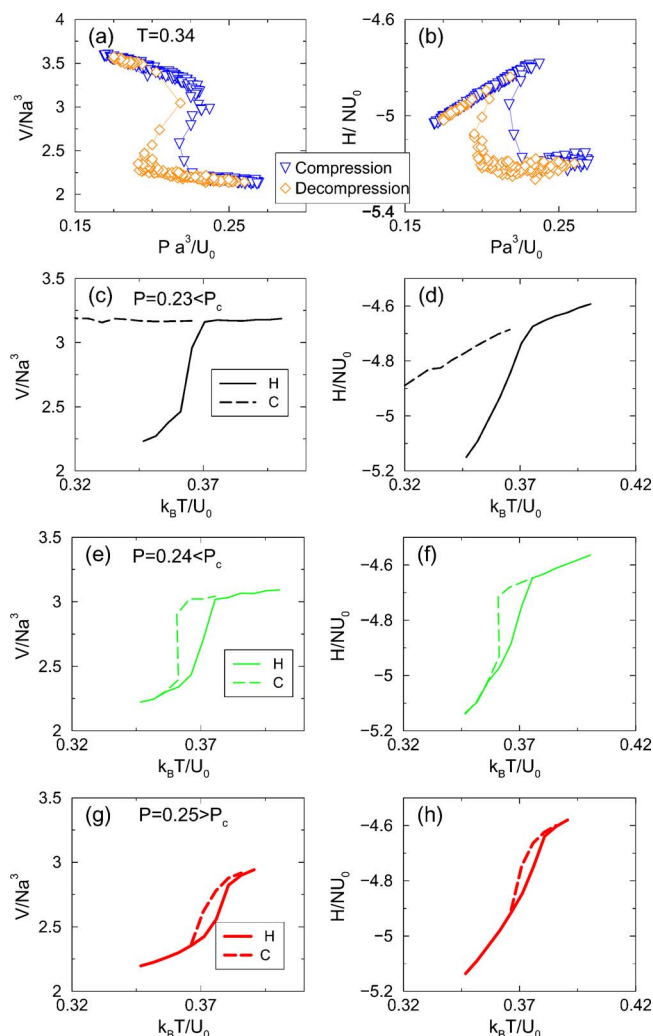


FIG. 3. (Color online) (a) Volume per particle (V/Na^3) and (b) enthalpy per particle (H/NU_0) showing hysteresis upon compression and decompression along a constant temperature path with $T=0.34$. Volume per particle [panel (c), (e), (g)] and enthalpy per particle [panel (d), (f), (h)] showing hysteresis upon cooling (C) and heating (H) along constant pressure paths. The sharp difference between $P=0.23$ and $P=0.25$ corresponds to the fact that $P=0.23$ is below P_c (path β in Fig. 5), while $P=0.25$ is above P_c (path α in Fig. 5).

that the HDL phase loses its stability and spontaneously changes into the LDL in the vicinity of the HDL spinodal line [Fig. 4]. The LL critical point of the Jagla ramp model, in contrast to those of water and silicon models, lies well above the equilibrium melting line [Fig. 2] at which the solid and liquid phases coexist and are in equilibrium. We estimate the equilibrium melting temperature as the temperature at which the slab of the hcp crystal, obtained by spontaneous crystallization at low temperature, is at equilibrium with a slab of liquid for a given pressure. Note that the slope of the melting line, defined by Eq. (12), is negative since the specific volume of the hcp crystal is larger than the volumes of the HDL and LDL. Moreover, the slope changes sharply from a larger absolute value in the LDL to a smaller absolute value in the HDL as it crosses the coexistence line between

the HDL and the LDL, due to the fact that the entropy difference between crystal and the HDL phase is smaller than the entropy difference between crystal and the LDL phase, but the difference in volume between the crystal and the HDL is larger than the difference between the crystal and the LDL. Very recently, Gibson and Wilding [46] studied the family of Jagla ramp potentials with decreasing soft-core distance and found that there is a parameter range within which the critical point lies below the crystallization line, and the coexistence line has a negative slope, resembling the situation for water.

B. Density anomaly

The temperature of maximum density (TMD) line is defined by $(\partial V/\partial T)_P=0$. Due to the general thermodynamic relation

$$\left(\frac{\partial V}{\partial T}\right)_P = -\left(\frac{\partial P}{\partial T}\right)_V \left(\frac{\partial V}{\partial P}\right)_T, \quad (13)$$

the TMD line coincides with the locus of points satisfying $(\partial P/\partial T)_V=0$, which defines the pressure minimum on each isochore (Fig. 2). The density anomaly (density increase upon heating along constant pressure paths) can also be seen in the inset of Fig. 4.

C. Thermodynamics

Different thermodynamic response functions such as C_P and K_T , which diverge at the critical point, have maxima at temperatures $T_{\max}(P)$, which can be regarded as temperatures on the extension of the coexistence line above the critical temperature (the Widom line [5]) as we cool the system at constant pressure $P > P_c$ [47–50]. The simulated phase diagram based on the equation of state [Fig. 2] is shown in Fig. 5. We investigate C_P and K_T in the Jagla ramp model along paths α and path β (Fig. 5). We find that, along paths α , C_P has a maximum at $T_{\max}(P)$ [Fig. 6(a)], while K_T has a maximum at a slightly different $T_{\max}(P)$ [Fig. 6(b)]. The response functions— C_P and K_T —increase continuously along path β [Fig. 5] before the system reaches the stability limit near the LDL spinodal [21].

D. Structural order

Analogously, we can expect that the structural properties of the system also change from those resembling the LDL phase to those resembling the HDL phase when the system crosses the Widom line. The pair correlation function $g(r)$ for different T along a constant pressure path is shown in Fig. 7(a). At low temperature $g(r)$ exhibits a more pronounced first peak near the hard core distance and a less pronounced peak at high T , indicating a change from the LDL-like structure to HDL-like structure upon cooling along paths α . The same behavior can also be seen from the static structure factor $S(q)$ [Fig. 7(b)]. The sharp transition in the translational order parameter t [Fig. 7(c)] and the peaks in the orientational order parameter Q_6 [Fig. 7(d)] above the LL critical point along path α , indicate that as the system crosses

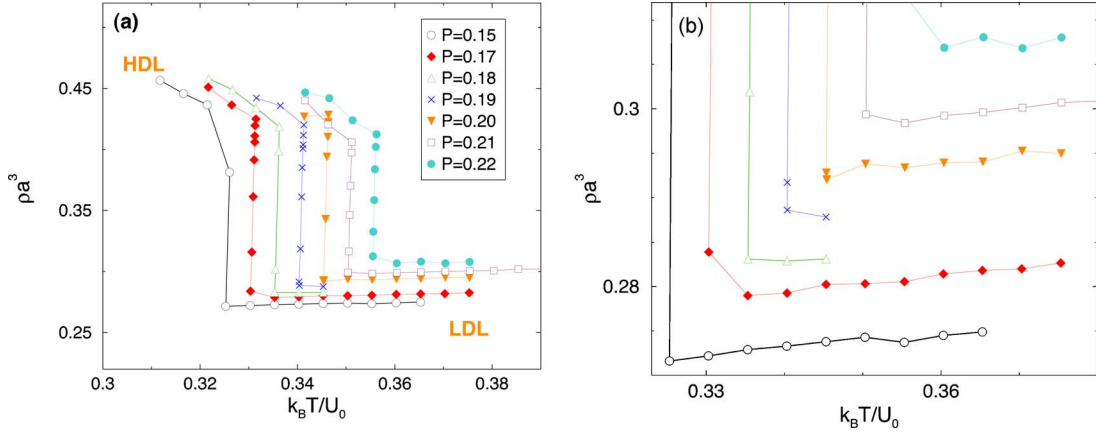


FIG. 4. (Color online) Liquid-liquid phase transition for the two-scale Jagla ramp potential. Upon heating along constant pressure paths below the critical point $P=P_c \approx 0.243$ [path β in Fig. 5], the system experiences a HDL to LDL phase transition near the HDL spinodal line. (b) The density anomaly upon heating along the same constant pressure paths.

the Widom line region [Fig. 5], the local structure of the system also changes from LDL-like to HDL-like, which is consistent with the features observed in the thermodynamic response functions.

VI. SIMULATION RESULTS: DYNAMICS

A. Diffusivity anomaly

Figure 8 shows the diffusivity $D(\rho)$ along seven isotherms. There exists a diffusivity anomaly region along each

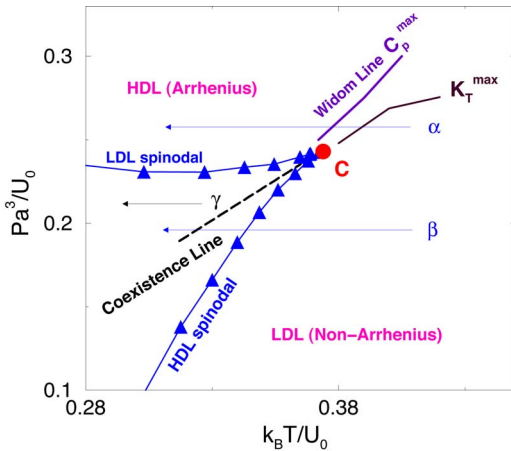


FIG. 5. (Color online) The P - T phase diagram for the two-scale Jagla ramp model. The loci of the specific heat maximum C_p^{\max} and the compressibility maximum K_T^{\max} are similar, but not identical. We study three different paths in the vicinity of the LL critical point: (i) $P > P_c$ (path α). Upon cooling along path α , the liquid changes from a low density state (characterized by a non-Arrhenius dynamic behavior) to a high density state (characterized by Arrhenius dynamic behavior) as the path crosses the Widom line. (ii) $P < P_c$ (path β). Upon cooling along path β , the liquid remains in the LDL phase as long as path β does not cross the LDL spinodal line. Thus one does not expect any dramatic change in the dynamic behavior along the path β . (iii) $P < P_c$ (path γ). Upon cooling along path γ , the liquid remains in HDL phase. Its dynamics, different from that of the LDL phase, follows Arrhenius behavior.

isotherm where the diffusivity *increases* upon compressing instead of decreasing. The loci of the diffusivity extrema where $(\partial D / \partial P)_T = 0$ [heavy dashed lines in Fig. 2 and Fig. 8] define the diffusivity anomaly region.

We study the T dependence of D along three different constant pressure paths [Fig. 5]: (i) Path α , $P > P_c$ (one-phase region); (ii) path β , $P < P_c$ (in the LDL phase); and (iii) path γ , $P < P_c$ (in the HDL phase).

B. Dynamics for $P < P_c$

For $P < P_c$, the diffusivity D at high temperature $T > T_c$ follows the Arrhenius law

$$D = D_0 \exp\left(-\frac{E_A}{k_B T}\right) \quad (14)$$

with a roughly pressure independent activation energy $E_A \approx 1.53$, while at low temperatures in the two-phase region, D behaves differently along path β and path γ upon cooling at constant pressure [Fig. 9]. Along path β [Fig. 5] which belongs to the LDL phase, the T dependence of D is non-Arrhenius and follows the Vogel-Fulcher-Tamann law

$$D = D_0 \exp\left(-\frac{B}{T - T_0}\right) = D_0 \exp\left(-\frac{T_0}{T - T_0} \frac{1}{f}\right). \quad (15)$$

For $P=0.225$, the fitting parameters are $B \approx 0.2$, $T_0 \approx 0.184$, and the fragility parameter $f = T_0/B \approx 0.66$ [Fig. 9]. Following Ref. [51], we estimate the glass transition temperature $T_g = 0.192$, defined as the temperature at which $\exp[B/(T - T_0)] = 10^k$ with $k = 16$, a typical value for thermally activated system. The fragility index m [51], defined as the slope of the Arrhenius plot at T_g , is approximately 368. This large value of m indicates that the behavior in the LDL phase resembles that of a very fragile liquid. Note that the value of the index number m largely depends on the Vogel-Fulcher-Tamman fitting at the last data point [Fig. 9(a)].

On the other hand, along paths γ which belong to the HDL phase, D follows Arrhenius behavior with $E_a \approx 6.30$, which is much larger than the activation energy at high temperature.

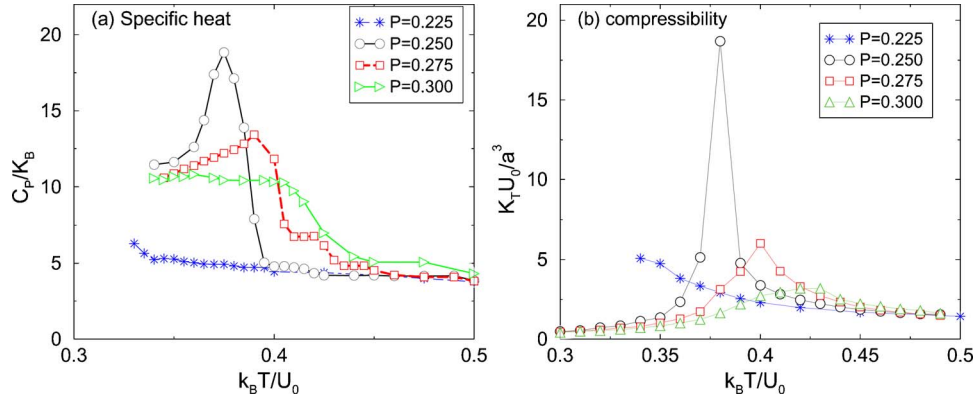


FIG. 6. (Color online) Response functions for the Jagla ramp model as function of temperature for different values of $P > P_c$ [Fig. 5, path α] and $P < P_c$ [Fig. 5, path β]. (a) Constant pressure specific heat C_p and (b) isotherm compressibility K_T . Both C_p and K_T have maxima, as is known to occur experimentally for the liquid-gas critical point [47] and for the liquid-liquid critical point [55]. For large P the peaks become less pronounced and shift to higher temperature as the Widom line has positive slope.

C. Dynamics for $P > P_c$

For $P > P_c$ along path α , there is a crossover in the behavior of D near $T \approx 0.4$ [Figs. 9(b) and 9(c)]. Such a crossover in the vicinity of the specific heat maximum is consistent with the Adam-Gibbs equation [52],

$$D = D \exp\left(-\frac{C}{TS_{conf}}\right), \quad (16)$$

where S_{conf} is the configurational entropy. Due to a proportionality between S_{conf} and S_{ex} [17] which is the excess entropy of liquid over crystal, the Adam-Gibbs equation has been used successfully in a number of experimental studies

with S_{conf} replaced by S_{ex} [17]. Indeed, since $C_p = T(\partial S/\partial T)_p$ and $C_p \propto C_p^{ex} \equiv T(\partial S_{ex}/\partial T)_p$, one can expect rapid change of the entropy near the temperature of maximum specific heat, and the same change for the configurational entropy which constitutes the major contribution to the excess entropy. When C_p has fallen to a smaller and more slowly changing value, the temperature dependence of D assumes an Arrhenius behavior but with a somewhat larger slope than at high temperatures where Fig. 6(a) shows C_p to be very small. The behavior is similar to what was observed in experimental studies of the strong liquid BeF_2 [53] and in simulations of SiO_2 [16]. In fact, the parallel with the case of BeF_2 [53] is remarkable. In both cases, the Arrhenius slope

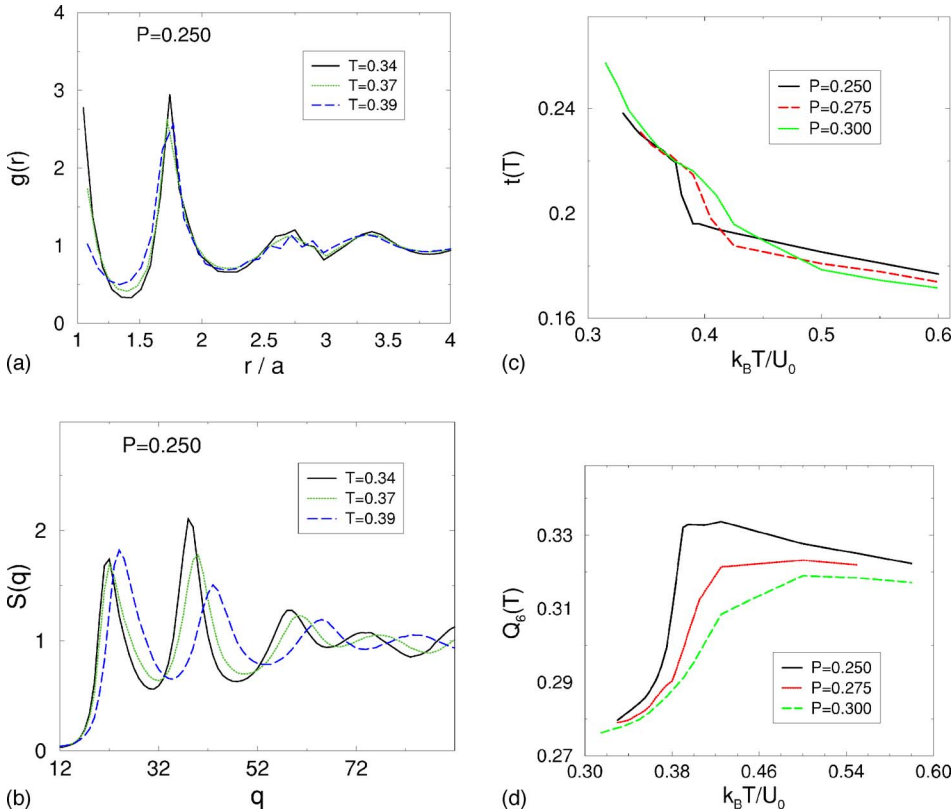


FIG. 7. (Color online) (a) The pair correlation function $g(r)$ at constant pressure $P=0.250 > P_c$. The magnitude of the first peak indicates a HDL-like liquid at low T and LDL-like liquid at high T . (b) Distribution of q vectors at constant pressure $P=0.250$. The shifts of the first and second peaks in the distribution of the q vectors further indicates that the liquid changes smoothly from HDL-like to LDL-like as it crosses the Widom line at temperature $T_w \approx 0.38$. (c) The translational order parameter t and (d) the orientational order parameter Q_6 along the constant pressure paths for $P > P_c$ [Fig. 5], path α . The sudden change in t and Q_6 occurs when the system crosses the positively sloped Widom line.

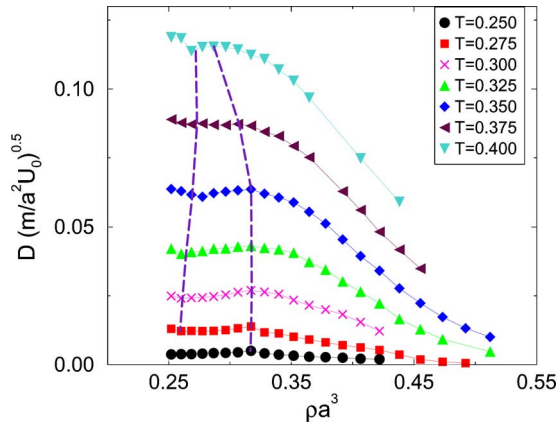


FIG. 8. (Color online) Dimensionless diffusivity as a function of density for seven values of temperature. The diffusivity anomaly region, where D increases with compression (density), is located within the diffusivity extrema lines (heavy dashed lines).

extrapolates to an intercept at $1/T=0$, which is six orders of magnitude above the intercept of the high temperature Arrhenius part of the plot (which is common to all phases). Thus, the behavior of the HDL-like liquid on the low-temperature side of the Widom line can be classified as that of a strong liquid. The behavior on the high-temperature side of the Widom line, in the LDL-like phase, however, is very different, resembling that of the fragile liquid, as is clear from Figs. 9(b) and 9(c). Thus, the present spherically symmetric Jagla ramp potential exhibits a dynamic crossover from LDL-like (fragile liquid) at high temperature to HDL-like (strong liquid) at low temperature, suggesting the analogous fragile-to-strong transition as in water, with the difference that the strong liquid is now the HDL phase.

VII. DISCUSSION

A. Jagla ramp potential

The mechanisms underlying the different dynamic behaviors we find can be related to the LL phase transition [Fig. 5]. The coexistence line has a positive slope, so we have one phase for $P > P_c$ and two phases—LDL and HDL—for $P < P_c$. According to the Clapeyron equation, HDL entropy is lower than LDL entropy, so HDL is more ordered than LDL which is the opposite of water. In the region of the P - T phase diagram between the LDL and HDL spinodals, the system can exist in both the LDL and HDL phases, one stable and one metastable.

(i) The limit of stability of the less-ordered LDL phase is determined by the high pressure LDL spinodal $P_{LDL}(T)$, which, for our model, is unlikely to be crossed by cooling the system at constant pressure [Figs. 3(c) and 3(d)]—because $P_{LDL}(T) \approx P_c$ for all T except in the immediate vicinity of the liquid-liquid critical point [Fig. 5]. The dynamic behavior of the less ordered LDL phase is non-Arrhenius, which is the characteristic of fragile glass formers [Fig. 5].

(ii) On the other hand, the limit of stability of the more ordered HDL phase is determined by the low pressure HDL

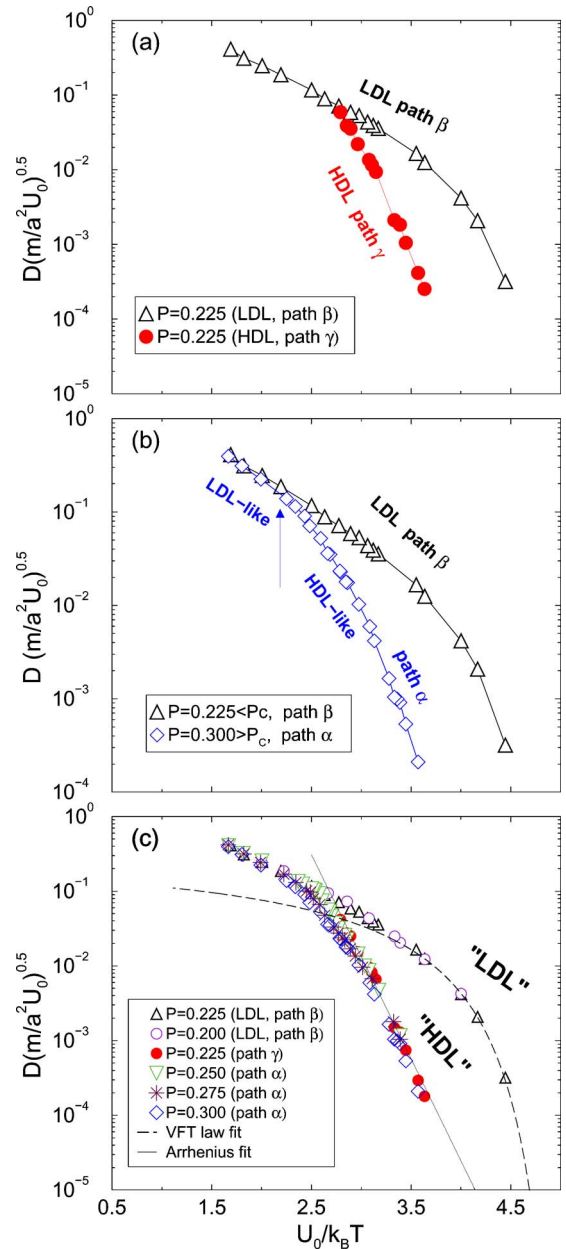


FIG. 9. (Color online) Dynamic behavior for Jagla ramp potential. The T dependence of the diffusivity D along constant pressure paths: (a) $P=0.225 < P_c$ for both path β and path γ . The more ordered phase (HDL) is strong, while the less ordered phase (LDL) is fragile. (b) Path β with $P=0.225 < P_c$, and path α with $P=0.300 > P_c$, for which a dynamic crossover occurs along constant pressure paths above the critical pressure when the Widom line is crossed [Fig. 5]. (c) Path β with $P=0.200, P=0.225 < P_c$, path γ with $P=0.225 < P_c$, and path α with $P=0.250, 0.275, 0.300 > P_c$.

spinodal $T_{HDL}(P)$ [Fig. 5], which can be crossed by heating the HDL phase at constant pressure [Figs. 3(c) and 3(d)]. That is why the dynamic behavior of the more ordered HDL phase can be studied only when $T < T_{HDL}(P)$ for $P < P_c$. The dynamic behavior of the HDL phase is Arrhenius which is the characteristic of the strong glass formers.

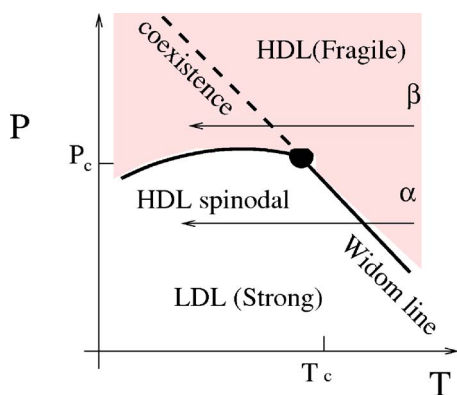


FIG. 10. (Color online) A sketch of the P - T phase diagram for water models, showing path α and path β [5]. Note that unlike the Jagla two-scale ramp potential [Fig. 5], the HDL is *less* ordered than the LDL, so the Widom line has negative slope by the Clapeyron relation.

B. Comparison with water

For the Jagla ramp model, the dynamic crossover upon cooling for $P > P_c$ (path α) is the same as what was observed in realistic water models for $P < P_c$ [3,14], which is a fragile to strong transition. In water models which have a negatively sloped coexistence, the density of the high temperature phase is larger than the density of the low temperature phase [Fig. 10]. Accordingly, the coexistence line has a negative slope, and the high temperature phase which must be the less ordered phase is the HDL phase [54]. Thus in water, in contrast with the Jagla model, the HDL phase is fragile while the LDL phase is strong. When water is cooled at $P > P_c$ [Fig. 10, path β], it crosses the coexistence line but does not cross the spinodal of the less ordered HDL phase, which is an almost horizontal line on the P - T plane as recent $ST2$ simulations suggest [2]. Thus for $P > P_c$, water may remain in the metastable HDL phase even at very low temperatures, since the low-density phase may not nucleate out of the HDL phase. Accordingly, above the critical pressure, water may remain fragile even at very low temperatures. In contrast, upon cooling at $P < P_c$ [Fig. 10, path α], water crosses the Widom line, and its thermodynamic properties continuously change from those of the HDL phase to those of the LDL phase. This is demonstrated by the C_p peak found by cooling water in small pores at atmospheric pressure [55]. Therefore, for $P < P_c$ one expects a fragile-to-strong transition upon cooling, which is indeed experimentally observed in nanopores [3,4].

C. Comparison with the tetrahedral liquid BeF_2

Interestingly, what was observed in a combined MD/experimental study of BeF_2 [53,56,57] shows a dynamic crossover similar to what we observed for Jagla ramp model

for $P > P_c$ [Fig. 9(a)]. In addition, the MD simulations of BeF_2 show the density anomaly and the specific heat maximum close to the point of the dynamic crossover at about $2T_g$. In the Jagla ramp model, the dynamic crossover and the C_p maximum occur at higher temperatures $T \approx 3.5T_g$. The difference between BeF_2 and the Jagla ramp model is that a second LL critical point has not been directly observed for BeF_2 . Therefore, we cannot call the region of fast change of the dynamic and thermodynamic properties a Widom line. However, the extrapolation of the simulation isochores in the density anomaly region suggests possible existence of a critical point at lower temperature and higher pressure. Thus, the region of fast changes of the thermodynamic response functions is possibly associated with a Widom line emanating from this hypothetical critical point [58,59] inaccessible for simulations. As in water, this region in BeF_2 (quasi-Widom line) has negative slope, suggesting that the dynamic crossover in BeF_2 upon cooling is related to the entropy decrease from a HDL-like value on the high-temperature side to a LDL-like value on the low-temperature side of this quasi-Widom line.

VIII. SUMMARY

In summary, we systematically study a simple spherically symmetric two-scale Jagla ramp potential with both repulsive and attractive parts. We find a LL phase transition in an accessible region of the P - T phase diagram. The Jagla ramp potential also displays water-type thermodynamic and dynamic anomalies, as well as a dynamic crossover which occurs as the system crosses the Widom line while cooled along constant pressure paths $P > P_c$. Our simulations, similar to simulations of silicon [18], show that the dynamics is Arrhenius in the more ordered phase (HDL for Jagla ramp model) and fragile for the less ordered phase (LDL for Jagla ramp model). Our study shows that the dynamics is Arrhenius on the low-temperature side of the Widom line and fragile on the high-temperature side of the Widom line, as in water. The dynamic crossover for $P > P_c$ is consistent with (i) the experimental observation in confined geometries (small pores) of a fragility transition [3], and (ii) experimental observation of a peak in the specific heat upon cooling water at atmospheric pressure in nanopores [55].

ACKNOWLEDGMENTS

We thank S.-H Chen, D. Chandler, P. G. Debenedetti, I. Ehrenberg, G. Franzese, J. P. Garrahan, P. Kumar, J. M. H. Levelt Sengers, M. Mazza, P. H. Poole, F. Sciortino, S. Sastry, F. W. Starr, B. Widom, and Z. Yan for helpful discussions and NSF Grant No. CHE 0096892 for support. We also thank the Boston University Computation Center for allocation of CPU time. S.V.B thanks the Office of the Academic Affairs of Yeshiva University for funding the high-performance computer cluster.

- [1] P. H. Poole, F. Sciortino, U. Essmann, and H. E. Stanley, *Nature (London)* **360**, 324 (1992); P. H. Poole, F. Sciortino, U. Essmann, and H. E. Stanley, *Phys. Rev. E* **48**, 3799 (1993); P. H. Poole, U. Essmann, F. Sciortino, and H. E. Stanley, *ibid.* **48**, 4605 (1993); F. Sciortino, P. H. Poole, U. Essmann, and H. E. Stanley, *ibid.* **55**, 727 (1997); O. Mishima and H. E. Stanley, *ibid.* **396**, 329 (1998).
- [2] P. H. Poole, F. Sciortino, T. Grande, H. E. Stanley, and C. A. Angell, *Phys. Rev. Lett.* **73**, 1632 (1994).
- [3] A. Faraone, L. Liu, C.-Y. Mou, C.-W. Yen, and S.-H. Chen, *J. Chem. Phys.* **121**, 10843 (2004).
- [4] L. Liu, S.-H. Chen, A. Faraone, C.-W. Yen, and C.-Y. Mou, *Phys. Rev. Lett.* **95**, 117802 (2005).
- [5] L. Xu, P. Kumar, S. V. Buldyrev, S.-H. Chen, P. Poole, F. Sciortino, and H. E. Stanley, *Proc. Natl. Acad. Sci. U.S.A.* **102**, 16807 (2005); L. Xu, I. Ehrenberg, S. V. Buldyrev, and H. E. Stanley, *J. Phys.: Condens. Matter* **18**, S2239 (2006); P. Kumar, S. V. Buldyrev, and H. E. Stanley, in *Soft Matter under Extreme Pressures: Fundamentals and Emerging Technologies*, edited by Sylwester J. Rzoska and Victor Mazur [Proc. NATO ARW, Odessa, Oct. 2005] (Springer, Berlin, 2006).
- [6] F. M. Mallamace, M. Broccio, C. Corsaro, A. Faraone, U. Wanderlingh, L. Liu, C.-Y. Mou, and S.-H. Chen, *J. Chem. Phys.* **124**, 161102 (2006).
- [7] S.-H. Chen, L. Liu, E. Fratini, P. Baglioni, A. Faraone, and E. Mamontov, *Proc. Natl. Acad. Sci. U.S.A.* **103**, 9012 (2006).
- [8] S.-H. Chen, L. Liu, X. Chu, Y. Zhang, E. Fratini, P. Baglioni, A. Faraone, and E. Mamontov (unpublished).
- [9] P. Kumar, Z. Yan, L. Xu, M. G. Mazza, S. V. Buldyrev, S.-H. Chen, S. Sastry, and H. E. Stanley, e-print cond-mat/0603557.
- [10] V. Velikov, S. Borick, and C. A. Angell, *Science* **294**, 2335 (2001).
- [11] G. P. Johari, *J. Phys. Chem. B* **107**, 9063 (2003).
- [12] C. A. Angell, *Science* **267**, 1924 (1995).
- [13] C. A. Angell, *J. Phys. Chem.* **97**, 6339 (1993).
- [14] K. Ito, C. T. Moynihan, and C. A. Angell, *Nature (London)* **398**, 492 (1999).
- [15] R. Bergman and J. Swenson, *Nature (London)* **403**, 283 (2000).
- [16] I. Saika-Voivod, P. H. Poole, and F. Sciortino, *Nature (London)* **412**, 514 (2001).
- [17] F. W. Starr, C. A. Angell, and H. E. Stanley, *Physica A* **323**, 51 (2003).
- [18] S. Sastry and C. A. Angell, *Nat. Mater.* **2**, 739 (2003).
- [19] S.-H. Chen, F. Mallamace, C.-Y. Mou, M. Broccio, C. Corsaro, A. Faraone, and L. Liu, *Proc. Natl. Acad. Sci. U.S.A.* (to be published); P. Kumar, S. V. Buldyrev, and H. E. Stanley (unpublished).
- [20] P. Kumar, G. Franzese, and H. E. Stanley (unpublished).
- [21] P. G. Debenedetti, *Metastable Liquids: Concepts and Principles* (Princeton University Press, Princeton, 1996).
- [22] O. Mishima and H. E. Stanley, *Nature (London)* **392**, 164 (1998).
- [23] M. Yamada, S. Mossa, H. E. Stanley, and F. Sciortino, *Phys. Rev. Lett.* **88**, 195701 (2002).
- [24] P. G. Debenedetti, *J. Phys.: Condens. Matter* **15**, R1669 (2003); P. G. Debenedetti and H. E. Stanley, *Phys. Today* **56**, 40 (2003).
- [25] F. Sciortino, E. La Nave, and P. Tartaglia, *Phys. Rev. Lett.* **91**, 155701 (2003).
- [26] D. Paschek, *Phys. Rev. Lett.* **94**, 217802 (2005).
- [27] P. H. Poole, I. Saika-Voivod, and F. Sciortino, *J. Phys.: Condens. Matter* **17**, L431 (2005).
- [28] P. Kumar, S. V. Buldyrev, F. W. Starr, N. Giovambattista, and H. E. Stanley, *Phys. Rev. E* **72**, 051503 (2005).
- [29] F. H. Stillinger, *Chem. Phys.* **65**, 3968 (1976).
- [30] F. H. Stillinger and D. K. Stillinger, *Physica A* **244**, 358 (1997).
- [31] M. R. Sadr-Lahijany, A. Scala, S. V. Buldyrev, and H. E. Stanley, *Phys. Rev. Lett.* **81**, 4895 (1998); *Phys. Rev. E* **60**, 6714 (1999); A. Scala, M. R. Sadr-Lahijany, N. Giovambattista, S. V. Buldyrev, and H. E. Stanley, *J. Stat. Phys.* **100**, 97 (2000); *Phys. Rev. E* **63**, 041202 (2001).
- [32] E. A. Jagla, *J. Chem. Phys.* **111**, 8980 (1999); E. A. Jagla, *J. Phys. Chem.* **11**, 10251 (1999); *Phys. Rev. E* **63**, 061509 (2001).
- [33] S. V. Buldyrev, G. Franzese, N. Giovambattista, G. Malescio, M. R. Sadr-Lahijany, A. Scala, A. Skibinsky, and H. E. Stanley, in *New Kinds of Phase Transitions: Transformations in Disordered Substances*, NATO Advanced Research Workshop, Volga River, edited by V. Brazhkin, S. V. Buldyrev, V. Ryzhov, and H. E. Stanley (Kluwer, Dordrecht, 2002), pp. 97–120.
- [34] N. B. Wilding and J. E. Magee, *Phys. Rev. E* **66**, 031509 (2002).
- [35] P. Kumar, S. V. Buldyrev, F. Sciortino, E. Zaccarelli, and H. E. Stanley, *Phys. Rev. E* **72**, 021501 (2005).
- [36] P. C. Hemmer and G. Stell, *Phys. Rev. Lett.* **24**, 1284 (1970); G. Stell and P. C. Hemmer, *J. Chem. Phys.* **56**, 4274 (1972); J. M. Kincaid and G. Stell, *ibid.* **67**, 420 (1977); J. M. Kincaid, G. Stell, and E. Goldmark, *ibid.* **65**, 2172 (1976); J. M. Kincaid, G. Stell, and C. K. Hall, *ibid.* **65**, 2161 (1976).
- [37] G. Franzese, G. Malescio, A. Skibinsky, S. V. Buldyrev, and H. E. Stanley, *Nature (London)* **409**, 692 (2001).
- [38] P. A. Netz, S. V. Buldyrev, M. C. Barbosa, and H. E. Stanley, *Phys. Rev. E* **73**, 061504 (2006); A. B. de Oliveira, P. A. Netz, T. Colla, and B. C. Barbosa, *J. Chem. Phys.* **124**, 084505 (2006).
- [39] J. R. Errington and P. G. Debenedetti, *Nature (London)* **409**, 318 (2001).
- [40] D. C. Rapaport, *The Art of Molecular Dynamics Simulation* (Cambridge University Press, Cambridge, 1995).
- [41] S. V. Buldyrev and H. E. Stanley, *Physica A* **330**, 124 (2003).
- [42] A. Skibinsky, S. V. Buldyrev, G. Franzese, G. Malescio, and H. E. Stanley, *Phys. Rev. E* **69**, 061206 (2004); G. Malescio, G. Franzese, A. Skibinsky, S. V. Buldyrev, and H. E. Stanley, *ibid.* **71**, 061504 (2005).
- [43] S. V. Buldyrev, G. Franzese, N. Giovambattista, G. Malescio, M. R. Sadr-Lahijany, A. Scala, A. Skibinsky, and H. E. Stanley, *Physica A* **304**, 23 (2002).
- [44] H. J. C. Berendsen *et al.*, *J. Chem. Phys.* **81**, 3684 (1984).
- [45] Z. Yan, S. V. Buldyrev, N. Giovambattista, and H. E. Stanley, *Phys. Rev. Lett.* **95**, 130604 (2005); Z. Yan, S. V. Buldyrev, N. Giovambattista, P. G. Debenedetti, and H. E. Stanley, *Phys. Rev. E* **73**, 051204 (2006).
- [46] H. M. Gibson and N. B. Wilding, *Phys. Rev. E* **73**, 061507 (2006).
- [47] M. A. Anisimov, J. V. Sengers, and J. M. H. Levelt Sengers, in *Aqueous System at Elevated Temperatures and Pressures: Physical Chemistry in Water, Steam and Hydrothermal Solutions*, edited by D. A. Palmer, R. Fernandez-Prini, and A. H.

- Harvey (Elsevier, Amsterdam, 2004).
- [48] J. M. H. Levelt, Ph.D. thesis, University of Amsterdam, 1958 (unpublished).
- [49] A. Michels, J. M. H. Levelt, and G. Wolkers, *Physica (Amsterdam)* **24**, 769 (1958).
- [50] A. Michels, J. M. H. Levelt, and W. de Graaff, *Physica (Amsterdam)* **24**, 659 (1958).
- [51] The parameter m is defined in R. Böhmer, K. L. Ngai, C. A. Angell, and D. J. Plazek, *J. Chem. Phys.* **99**, 4201 (1993).
- [52] G. Adam and J. H. Gibbs, *J. Chem. Phys.* **43**, 139 (1965).
- [53] M. Hemmati, C. T. Moynihan, and C. A. Angell, *J. Chem. Phys.* **115**, 6663 (2001).
- [54] G. Franzese and H. E. Stanley, *J. Phys.: Condens. Matter* **14**, 2201 (2002); G. Franzese, M. I. Marqués, and H. E. Stanley, *Phys. Rev. E* **67**, 011103 (2003).
- [55] S. Maruyama, K. Wakabayashi, and M. Oguni, *AIP Conf. Proc.* **708**, 675 (2004).
- [56] S. V. Nemilov, G. T. Petrovskii, and L. A. Krylova, *Inorg. Mater.* **4**, 1453 (1968).
- [57] C. T. Moynihan and S. Cantor, *J. Chem. Phys.* **48**, 115 (1968).
- [58] V. V. Brazhkin, A. G. Lyapin, S. V. Popova, and R. N. Voloshin, in *New Kinds of Phase Transitions: Transformations in Disordered Substances*, NATO Advanced Research Workshop, Volga River, edited by V. Brazhkin, S. V. Buldyrev, V. Ryzhov, and H. E. Stanley (Kluwer, Dordrecht, 2002), pp. 15–28.
- [59] V. V. Brazhkin, R. N. Voloshin, S. V. Popova, and A. G. Lyapin, in *New Kinds of Phase Transitions: Transformations in Disordered Substances*, NATO Advanced Research Workshop, Volga River, edited by V. Brazhkin, S. V. Buldyrev, V. Ryzhov, and H. E. Stanley (Kluwer, Dordrecht, 2002), pp. 239–254.